Speckled Images Segmentation and Algorithm Comparison

Luigi Cinque[1], Rossella Cossu[2] and Rosa Maria Spitaleri[2]
[1]*Dipartimento Informatica, Universitá degli Studi, Sapienza, Via Salaria 113, 00185 Roma, Italy*
[2]*Istituto per le Applicazioni del Calcolo-CNR, Via dei Taurini 19, 00185 Roma, Italy*

Keywords: Speckle, Image Segmentation, Level Set, Partial Differential Equation.

Abstract: An image segmentation process, based on the level set method, consists in the time evolution of an initial curve until it reaches the boundary of the objects to be extracted. Classically the evolution of the initial curve is determined by a speed function. In this paper, the speed in the level set procedure is characterized by the combination of two different speed functions and the resulting algorithm is applied to speckled images, like SAR (Synthetic Aperture Radar) images. In order to assess improvements of the segmentation performance, the computational process is tested on synthetic and then applied to real images. Performances are evaluated on synthetic images by using the Hausdorff distance. The real SAR images were acquired during the ERS2 mission.

1 INTRODUCTION

We face the problem of speckled images segmentation, like the SAR images. It is well known that the presence of speckle, modeled as a strong multiplicative noise, makes regions detection a very complicated issue.

In the last decades, variational methods, based on the $\Gamma - convergence$ property (Mumford and Shah, 1989), (Spitaleri, March and Arena,1999), (Cinque, Cossu and Spitaleri, 2014) or the level set approach, (Sethian, 1999), (Sethian, 2001),(Osher and Fedkiw, 2002) (Cinque and Cossu, 2011) leading to solve partial differential equations (PDEs), have been important tools for solving image segmentation problems.
References show that we have been developing variational segmentation algorithms by both approaches. The level set segmentation is characterized by the implicit representation of a curve that evolves over time, defined as the zero level of a 3D level function (Sethian, 1999), (Sethian, 2001),(Osher and Fedkiw, 2002).

Active contours methods had a fundamental role in image segmentation. They are computer generated curves that move within the image to find the the boundaries of the regions under the influence of internal and external forces (Kass, Witkin and Terzopulos, 1988) (Chan and Vese, 2001). The evolution of the curve is carried out in accordance with a speed function, fundamental step to achieve a good segmentation.

In this paper we present a new speed, which is the linear combination of two different speed functions: the first speed, called average-based speed (Ben Ayed, Mitiche and Belhadj, 2005), (Mitiche and Ben Ayed, 2011) (Ben Salah, Ben Ayed and Mitiche, 2012) depends on the mean gray values of the two regions, foreground and background, identified by the curve, the second speed, called gradient-based speed, depends on the image gradient previously processed with a SRAD (Speckle Reducing Anisotropic Diffusion) filter (Yongjian and Acton, 2002) to reduce the speckle noise.

We compare the results of the segmentation obtained applying the level set equation with the new combined speed either the average-based or the gradient-based speed separately. Our approach is validated by tests on synthetic speckled images; in particular by calculating the Hausdorff distance between the real contours and computed ones, we compare results in quantitative way (Huttenlocher, Klanderman and Rucklidge, 1993).

The Hausdorff distance measures the maximum of minimum distances between two subsets in a metric space, in our case between the sets of points belonging to the known and the computed contours of the test images.
We present and discuss results related to one or more objects, with non convex boundaries, corrupted by speckle noise, test images and SAR images. The SAR PRI (Precision Images)images here segmented were acquired during ERS2 mission. ERS2 SAR system is

Cinque L., Cossu R. and Maria Spitaleri R..
Speckled Images Segmentation and Algorithm Comparison.
DOI: 10.5220/0005166901110118
In *Proceedings of the International Conference on Pattern Recognition Applications and Methods* (ICPRAM-2015), pages 111-118
ISBN: 978-989-758-077-2

capable of 25 m. resolution from an altitude of 800 km, at radar wavelength of 5.7 cm.

The paper is organized as follows. In Section 2, the level set method is briefly described. In Section 3, speed computation related to level set method is introduced. In Section 4, experimental results, performance evaluation on test problems and application to SAR images are shown. Some conclusions are drawn in Section 5.

2 MATHEMATICAL MODELING

The level set function is characterized by the implicit representation of a curve. It is defined as a signed distance function, where the points of the curve assume zero value, while at any other point the value of the function is given by the minimum distance between this point and the curve.

Since the image segmentation consists in the extracting the boundary of regions of interest from an image. This boundary may be considered as a curve belonging to a family whose time evolution is described by a level set equation. In order to resolve this equation, an iterative process computes the evolution of the initial curve corresponding to the resolution of the differential equation in partial derivatives.

2.1 Curve Evolution by Level Set

In order to obtain the governing equation of a front evolution we consider a family of parametrized closed contours (t is the parameter) $C(x(t),y(t),t) : [0,\infty) \rightarrow R^2$, generated by evolving an initial contour $C_0(x(0),y(0),0)$. We underline that in the curves evolution theory the geometric shape of the contour is determined by the normal component of the evolution velocity.

If $F(x(t),y(t),t)$ is a scalar function representing the curve speed in the normal direction $\vec{n}$, the normal velocity components are

$$\frac{dx}{dt} = F(x(t),y(t),t)\cdot n_1 \qquad \frac{dy}{dt} = F(x(t),y(t),t)\cdot n_2$$

with $\vec{n} \equiv (n_1,n_2)$. So that the curve evolves in time according to the following equation

$$\frac{\partial C(x(t),y(t),t)}{\partial t} = F(x(t),y(t),t)\cdot \vec{n} \qquad (1)$$

Supposing that $C(x(t),y(t),t)$ is a moving front in the image, if we embed this moving front as the zero level of a smooth continuous scalar 3D function $\phi(x(t),y(t),t)$, known as the level set function, the implicit contour at any time t is given by $C(x(t),y(t),t) \equiv \{(x(t),y(t))/\phi(x(t),y(t),t) = 0\}$.
By differentiating respect to t the expression $\phi(x(t),y(t),t) = 0$ the equation of motion for the level set function may be derived

$$\frac{\partial \phi(x(t),y(t),t)}{\partial t} + F(x(t),y(t),t)\cdot n_1 \frac{\partial \phi(x(t),y(t),t)}{\partial x} + \\ + F(x(t),y(t),t)\cdot n_2 \frac{\partial \phi(x(t),y(t),t)}{\partial y} = 0 \qquad (2)$$

Being now

$$n_1 = \frac{\frac{\partial \phi(x(t),y(t),t)}{\partial x}}{|\nabla \phi(x(t),y(t),t)|} \qquad n_2 = \frac{\frac{\partial \phi(x(t),y(t),t)}{\partial y}}{|\nabla \phi(x(t),y(t),t)|}$$

where $|\nabla \phi(x(t),y(t),t)| \neq 0$ for all $(x(t),y(t) \in C(x(t),y(t),t)$, the equation (2) becomes

$$\frac{\partial \phi(x(t),y(t),t)}{\partial t} + \frac{F(x(t),y(t),t)}{|\nabla \phi(x(t),y(t),t)|} + \\ \cdot[(\frac{\partial \phi(x(t),y(t),t)}{\partial x})^2 + (\frac{\partial \phi(x(t),y(t),t)}{\partial y})^2] = 0$$

Moreover for simplicity we can write $\mathbf{x} \equiv (x(t),y(t))$, $C \equiv C(x,y,t)$
or also

$$\frac{\partial \phi(\mathbf{x},t)}{\partial t} + F(\mathbf{x},t)|\nabla \phi(\mathbf{x},t)| = 0 \qquad (3)$$

In the following, an important intrinsic geometric property will be used, that is the curvature of level set (Sethian, 2001), is given by

$$k = -\nabla \cdot \left(\frac{\nabla \phi(\mathbf{x},t)}{|\phi(\mathbf{x},t)|}\right). \qquad (4)$$

2.2 Level Set Implementation

The numerical implementation of equation (3) is realized by performing a discretization with respect to time.
In the process of evolution of the curve, the level set function can lose the properties of the distance for the sake of approximation. To reduce calculation errors and ensure stability to the method, the function $\phi(\mathbf{x},t)$ is periodically re-initialized after a certain number of iterations.

The distance calculation is performed in the process of re-initialization, in order to transform the function $\phi(\mathbf{x},t)$ in a signed distance function (Li, Xu, Gui and Fox, 2010), by computing the current distance function.
In the implementation, for the numerical approximation of the level set equation in a domain $\Omega \subset \Re^2$

we introduce the computational domain Ω^* obtained by considering a uniform partition of Ω in $(N-1)\times(M-1)$ disjoint rectangles Ω_{ij} with edges $\Delta x = \Delta y$ which usually in an image are $\Delta x = \Delta y = 1$.
Let $P_{i,j} \equiv P(x_i, y_j)(i = 1,...,N; j = 1,...,M)$ be a point in Ω^* and $\phi^n_{i,j}$ the value of the function $\phi(\mathbf{x},t)$ at $P_{i,j}$ at time t^n.

The algorithm starts by initializing $\phi(\mathbf{x},t)$ as a signed distance function, depending on interior or external points of curve C

$$\phi(\mathbf{x}, t=0) = \pm d$$

where

$$d(\mathbf{x}) = \min_{\mathbf{x}_C \in C} |\mathbf{x} - \mathbf{x}_C|.$$

Now, known the value of $\phi^n_{i,j}$, the value $\phi^{n+1}_{i,j}$ is computed by a 2-order ENO scheme with the TVD (Total Variation Diminishing) Runge Kutta scheme for the time integration. The iterative process ends when the curve is stable or when it ceases its evolution, that is at convergence.

We underline that the definition of $\phi(\mathbf{x},t)$ as a signed distance function is crucial.
Moreover the choice of an appropriate speed function is a fundamental task for this segmentation approach. This function is computed by the original image, as it is described in the following section.

3 CURVE SPEED

In this section we present a synthetic introduction of the combined speed obtained by the contribution of the two speed functions (Cinque and Cossu, 2011). In this work we assume two types of regions, foreground and background, $R_i \quad i \in \{1,2\}$,
Let $I(\mathbf{x})$ be the SAR image intensity which is modeled by a Gamma distribution. After some probabilistic considerations and algebraic manipulations we obtain the average-based speed (Mitiche and Ben Ayed, 2011) in the form

$$\begin{aligned} F(\mathbf{x},t) &= \frac{dC}{dt} = \\ &= -\left(\log \mu_{R_1} + \frac{I(\mathbf{x})}{\mu_{R_1}} - \log \mu_{R_2} - \frac{I(\mathbf{x})}{\mu_{R_2}} + \lambda k\right) \end{aligned} \tag{5}$$

where λk is a regularization term, with $\lambda \in (0,1)$ and k the mean curvature function, μ_{R_i} is the mean intensity, with a_{R_i} the area of the region R_i, that is

$$\mu_{R_i} = \frac{\int_{R_i} I(\mathbf{x}) d\mathbf{x}}{a_{R_i}} \qquad a_{R_i} = \int_{R_i} d\mathbf{x}.$$

The gradient-based function is computed as the gradient magnitude of the original image and represents the front speed point by point (Cerimele, Cinque and Cossu, 2009).
It is well known that in images corrupted by strong noise, the computation of the gradient could detect false edges. For this reason, the speckle image is preprocessed by means of the SRAD algorithm which is an extension of Perona-Malik algorithm (Yongjian and Acton, 2002), (Perona and Malik, 1990).
The gradient-based speed (Sethian, 1999) is computed on the filtered image

$$F(\mathbf{x},t) = -\frac{1}{1+|\nabla I'(\mathbf{x})|^2} - \lambda k$$

where $I'(\mathbf{x})$ is the image $I(\mathbf{x})$ filtered by SRAD, k is the curvature and $\lambda \in (0,1)$ is a constant. So, the speed term is defined in such a way that the curve proceeds rather fast in low gradient zones, while it wades through to high gradient ones.
The new velocity is the linear combination of the average-based and gradient-based speed and it is given by the following expression:

$$\begin{aligned} F(\mathbf{x},t) = &-\alpha\left(\log\frac{\mu_{R_2}}{\mu_{R_1}} + I(\mathbf{x})\frac{\mu_{R_1}-\mu_{R_2}}{\mu_{R_1}\mu_{R_2}}\right) + \\ &-(1-\alpha)\left(\frac{1}{1+|\nabla I'(\mathbf{x})|^2}\right) - \lambda k. \end{aligned} \tag{6}$$

where $\alpha \in (0,1)$.
We can substitute the speed $F(\mathbf{x},t)$ (6) in the equation level set (3).
The function $\phi(\mathbf{x},t)$ is the computed contour of the extracted region at the convergence. The segmentation, indeed, is defined by the convergence for $t \to \infty$ of (3).
The procedure developed by using the combined speed improves the results obtained by the two speeds separately. We obtained the best results of segmentation setting, mainly, the parameter $\alpha = 0.5$.

4 EXPERIMENTAL RESULTS

In this section we apply the proposed algorithm to both synthetic and SAR images (Cinque and Cossu, 2011).

4.1 Application to Synthetic Images

We tested the procedure on synthetic images to have an exact reference of the contours to be detected .
In this paper, to evaluate the efficiency of the proposed speed, we calculated the Hausdorff distance between

the pixels of the known and computed contours of the synthetic images. Then we show the quantitative and qualitative comparison between resulting contours.
The Hausdorff distance H measures the maximum of minimum distances between the points of two contours. Given the contours $A = \{a_1, \ldots a_n\}$ and $B = \{b_1, \ldots b_n\}$, the Hausdorff distance is defined as

$$H(A,B) = \max(h(A,B), h(B,A))$$

where

$$h(A,B) = \max_{a \in A} \min_{b \in B} \|a - b\|$$

$\|a-b\|$ is any metric between the points of A and B (e. g.the Euclidean distance) (Huttenlocher, Klanderman and Rucklidge, 1993).
The following test image has been synthesized from an original image without noise, by copying a speckle pattern from SAR image.
Fig. 1 shows the images with the initial curve (a) and the corresponding results obtained by applying the level set equation, using the average-based speed (b), the gradient-based speed (c) and combined speed (d) respectively.
As recalled in Section 3, in the case of the computation of the gradient-based speed, the filter SRAD is applied to the image to preserve and enhance the edges (Yongjian and Acton, 2002). We solve (3) with (6), varying the parameter α, with $\alpha \in (0,1)$ and setting the parameter λ with $\lambda = 0.3$. We recall that $\lambda \in (0,1)$ and it indicates the weight, associated with the component speed that depends on the curvature k. Then the distance H between the known and computed contours is also computed for performance evaluation.

The results are the following:

- the chosen initial contour of Fig.1 (a) has the H distance from the real contour $H = 63.78$.
- the computed contour of Fig.1 (b), obtained by setting the parameter $\alpha = 0.9$, has the H distance from the real contour $H = 43.56$. As given by (6), the value $\alpha = 0.9$ implies a very low contribution of the gradient-based speed, thus we can note that this contour is mainly computed by average-based speed.
- the computed contour of Fig.1 (c), obtained by setting the parameter $\alpha = 0.1$, has the H distance from the real contour $H = 23.02$. In this case by (6), the value $\alpha = 0.1$ implies the very high contribution of gradient-based speed mainly. As above written, the level set equation is computed on the filtered image.

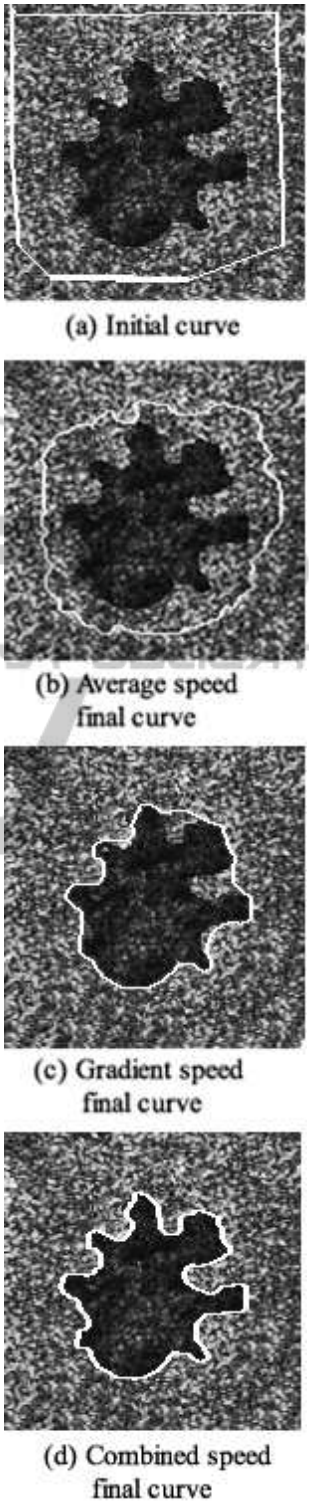

Figure 1: Speckled test image (150×150): (a) Starting contour, (b) final contour by average-based speed, (c) final contour by gradient-based speed, (d) final contour by combined speed.

- the computed contour of Fig. 1 (d), obtained by setting the parameter $\alpha = 0.5$, has the H distance from the known contour $H = 3.01$. $\alpha = 0.5$ determines the best result.

In this type of image the best results are computed, if the value of alpha is such that the contributions of the two speeds are similar, that is this α value balances the results of the two speeds.

In Fig. 2 we can see the result obtained from synthetic images constituted by background and three objects to be extracted. This image is corrupted by speckle noise of *variance* $= 0.2$. In Fig. 2, (a) and (b) the objects have the same gray levels, whereas (c) and (d) have three different gray levels. In Fig. 2, (b) and (d) the results have been obtained by setting $\alpha = 0.5$ and $\lambda = 0.3$.

In Fig. 3 we can see the overlapping of the results, in particular in Fig. 3 (a) the contours have a distance $H = 4$. and in Fig. 3 (b) $H = 7$.

4.2 Application to SAR Images

In this section we present some results performed by applying the combined procedure on SAR images acquired during ERS2 mission (2000).
ERS2 SAR system is capable of 25 m. resolution from an altitude of 800 km, at radar wavelength of 5.7 cm.

In Fig. 4 the SAR images, representing part of the coast of the Netherlands and a Baleari Island, are presented and the results obtained applying the level set procedure, based on combined speed, are shown.

In Fig. 4 (a) we notice an image with inhomogeneities regarding the intensity within the foreground. We used $\alpha = 0.6$ and $\lambda = 0.3$. The final result identifies three islands and the coast. In this case is important to underline that more objects are segmented also in SAR images. In Fig. 4 (b) we note an image with a granular aspect, small contrast between foreground and background. We used $\alpha = 0.5$ and $\lambda = 0.3$.
In Fig. 5 the result, obtained on a SAR image of 750×750 pixels, representing part of the coast of the Tuscan coast, is shown. The result is characterized by indented contour and by little islands and $\alpha = 0.5$ and $\lambda = 0.3$.

Fig. 6 shows the result obtained on a SAR image of 500×700 pixels depicting the Capraia Island for $\alpha = 0.3$ and $\lambda = 0.3$.

An example of indented contour is in Fig. 7, that shows the result obtained on a SAR image of 600×600 pixels representing part of the coast of Elba Island, setting $\alpha = 0.5$ and $\lambda = 0.3$

In the Fig. 8 (a) we present the image of size $200 \times$

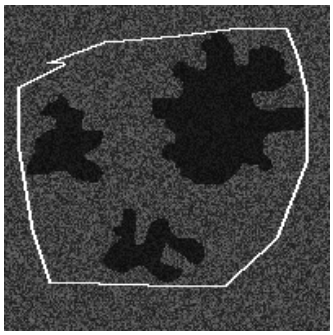

(a) Initial curve

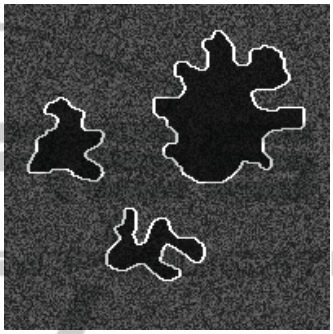

(b) Final Contours

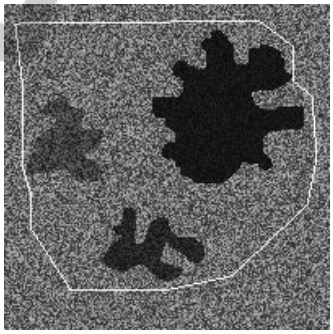

(c) Initial curve

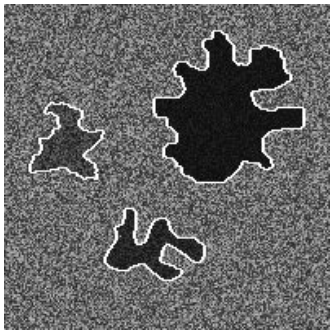

(d) Final contours

Figure 2: Speckled test images (200×200): (a) and(b)three objects of the same gray level, (c)and (d) of different gray levels

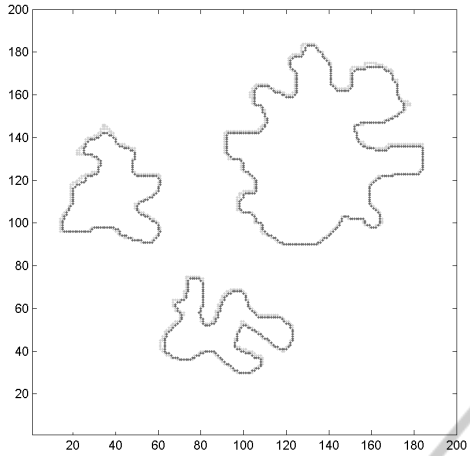

(a) H=4.

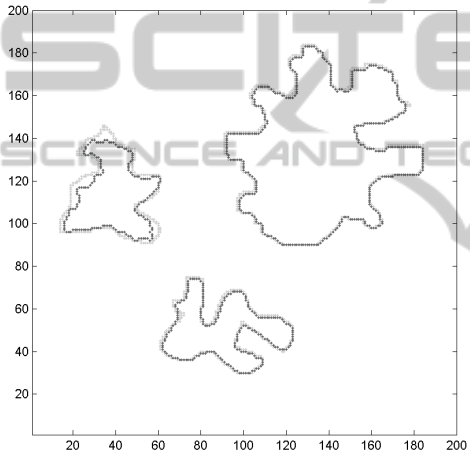

(b) H=7.

Figure 3: Hausdorff distance.

200 characterized by indented contour, representing the Netherlands coast. The white line is portion of the starting contour. The result of Fig. 8 (b) is obtained for $\alpha = 0.4$

The final results is more than satisfactory.

5 CONCLUSIONS

In this paper, we presented a level set segmentation algorithm applied to both synthetic and real SAR images and we discussed performance evaluation results.

The segmentation algorithm, based on a speed balancing both the average and the gradient speeds, works better than ones driven mainly by a single separated speed.

Combining two different speed functions for

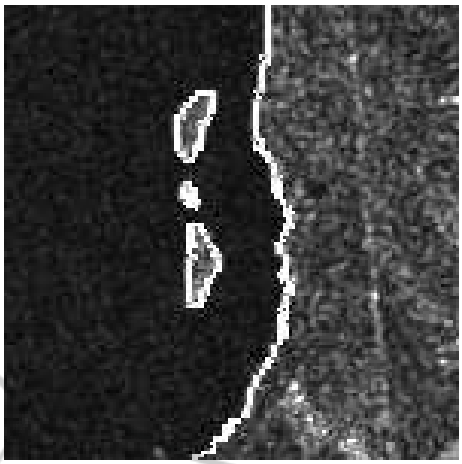

(a) Regular contours

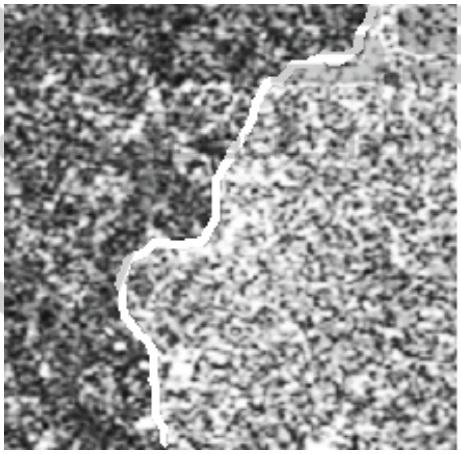

(b) Inhomogeneous background

Figure 4: Contours extraction of SAR images: (a) Netherlands coast and (b) Baleari coast.

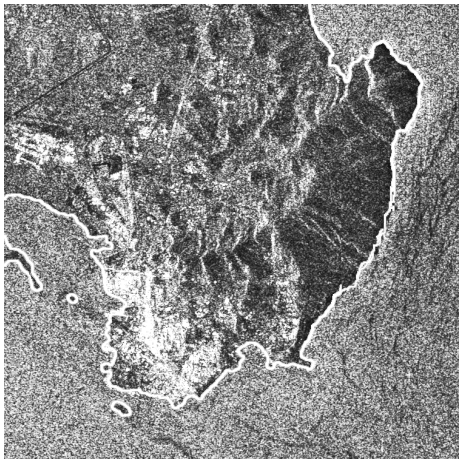

Figure 5: Contour extraction from the Tuscan image, $\alpha = 0.5$.

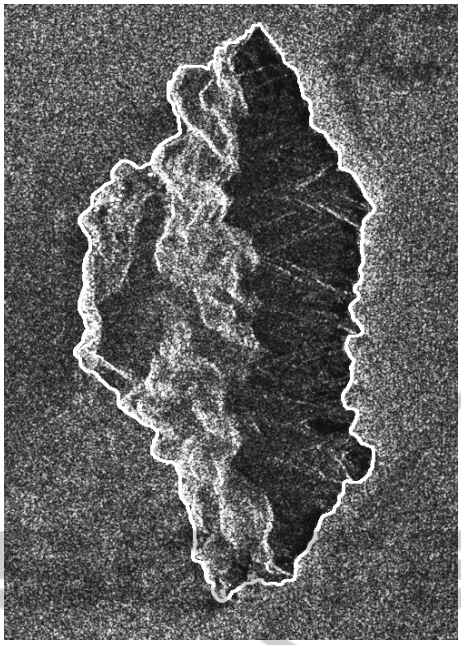

Figure 6: Contour extraction of the Capraia Island, $\alpha = 0.3$.

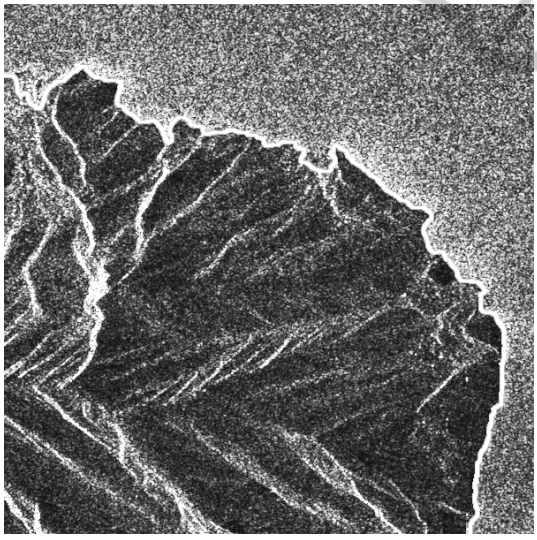

Figure 7: Resulting contour of the Elba Island, $\alpha = 0.5$.

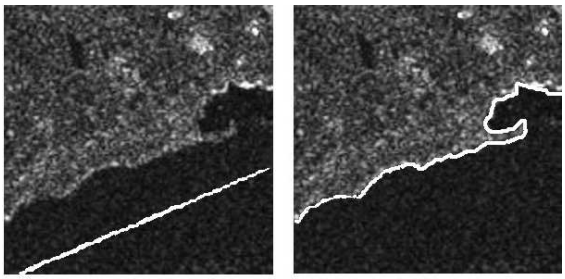

(a) Initial curve (b) Resulting contour

Figure 8: Extraction contour: (a) original image and starting contour, b) final contour, $\alpha = 0.4$.

curve evolution level set allows more accurate achievements of regions contours. We compared the results obtained applying the level set algorithm for the speckled test and real images segmentation. Results appear to be very promising for future developments.

In the future we plan to apply the proposed methodology to full resolution images obtained from (CSK) COSMO-SkyMed constellation. The constellation consists of 4 satellites, each one equipped with a microwave high-resolution synthetic aperture radar. It is the most important Italian event in the Space-Earth Observation environment in international field. We are going to test and validate the proposed procedure on images of the same regions acquired by different SAR systems.

REFERENCES

Cinque, L. and Cossu, R. (2011). Region segmentation from SAR images *Lectures Notes Computer Science* LNCS 6978 (ICIAP 2011), SPRINGER.

Sethian, J. A. (1999) *Level set methods and fast marching methods*, Cambridge University Press, 1999.

Sethian, J. A. (2001) Evolution, implementation and application of level set and fast marching methods for advancing front, *Journal of Computational Physics*, 169 (2001).

Osher, S. and Fedkiw, R. (2002) *Level set methods and dynamic implicit surfaces*, Springer-Verlag New York, 2002.

Ben Ayed, I. Mitiche, A. and Belhadj, Z. (2005), Multiregion level-set partitioning of synthetic aperture radar images, *IEEE Trans. Pattern Analysis and Machine Intelligence*, 27 (2005).

Mitiche, A. and Ben Ayed, I. (2011), *Variational and level set methods in image segmentation*, (2011) SPRINGER.

Ben Salah, M. Ben Ayed, I. and Mitiche, A. (2012), Active curve recovery of region boundary patterns, *IEEE Trans. Pattern Analysis and Machine Intelligence*, 34 (2012).

Yongjian, Yu and Acton Scott, T.(2002), Speckle reducing anisotropic diffusion, *IEEE Trans. on Image Processing*, 11 (2002).

Huttenlocher, D. Klanderman, G. and Rucklidge W. (1993) Comparing Images Using the Hausdorff Distance, *IEEE Trans. Pattern Analysis Machine Intelligence*,**15** (1993).

Mumford, D. and Shah, J. (1989), Optimal approximations by piecewise smooth functions and associated variational problems, *Comm. Pure Appl.Math.*, 42 (1989).

Spitaleri, R. M. March, R. and Arena D. (1999), Finite difference solution of Euler equation arising in variational image segmentation, *Numerical Algorithms*, 21 (1999).

Cinque, L. Cossu, R. and Spitaleri, R.M. (2014), Applied variational SAR image segmentation, *MASCOT12 & ISGG12 Proceedings, IMACS Series in Computational and Applied Mathematics*,18 (2014).

Chan, T. F. and Vese, L. A. (2001), Active Contours without edge, *IEEE Trans. on Image Processing*, 10 (2001).

Kass, M. Witkin, A. and Terzopoulos D. (2001), Snakes: active contour models, *Journal of Computational Vision*, 1 (1988).

Cerimele, M.M. Cinque, L. and Cossu, R. (2009), Coastline detection from SAR images by level set model, *Lectures Notes Computer Science* LNCS 5716 (ICIAP 2009), SPRINGER.

Perona, P. and Malik, J.,(1990) Scale space and edge detection using anisotropic diffusion, *IEEE Trans. Pattern Analysis and Machine Intelligence*, 12 (1990).

Li, C. Xu, C. Gui and Fox, D. (2010), Distance regularized level set evolution and its application to image segmentation, *IEEE Trans. on Image Processing*, 11 (2010).